Thermal Analysis of a Magnetic Packaged Power Module

Laili Wang, Doug Malcolm
Sumida Technologies Inc.
Sumida Corporation
Kingston, Canada
laili_wang@us.sumida.com

Wenbo Liu, Yan-Fei Liu *Fellow IEEE*
Department of Electrical and Computer Engineering
Queen's University,
Kingston, Canada
liu.wenbo@queensu.ca, yanfei.liu@queensu.ca

***Abstract*—Power density of converters have been dramatically increased through the innovations of packaging and integration technologies. Meanwhile, it also imposes more challenges on the thermal performances. An integrated power module packaged with magnetic component is proposed to improve both electrical and thermal performances. This paper presents the thermal analysis of the proposed power module. The magnetic component acts as both the filter inductor in the converter and the package of the power module. Benefiting from this package technology, the inductor can be designed with a bigger winding of lower resistance, thus generating less heat. The magnetic material has better thermal conductivity than plastic material used in conventional plastic packaged power modules; therefore, the power module has better thermal performance. Simulation is executed to show thermal effect of winding configurations. A thermal evaluation board is built to compare thermal performances of the proposed power module and two other commercial products. The proposed power module has 11℃ lower than the other part with the same size.**

Keywords—electrical packaging; thermal resistance; analytical model; finite element method

I. INTRODUCTION

Thermal performance is a significant issue in high power density converters from small power devices used as a power supply of a mother board to high power equipment used in wind turbine [1-10]. It is related to the efficiency, the materials of the components, and the package of the whole converter. In industry, it is a trend to increase the power density of the converters in electronic system with the purpose of reducing the total volume or leaving more space to integrate more functions. Different kinds of packaging and integration technology have been proposed to realize this purpose [2]. However, with the increased power density, the thermal issue becomes even more critical since either the total power is increased or the size of the converter is reduced. In some cases, extra measurements should be taken to dissipate the heat [4], which might impose adversary effect on increasing the power density. Besides, they can result in the increase of the total cost, too.

The integrated non-isolated power modules are the most popular DC/DC converters used in industry. They are widely used in telecom equipment, network servers, FPGAs, and other electronic devices. The input voltage rails can be 5V, 12V or even higher, the output voltage varies from 0.6V~5.5V. The output can be from hundreds of the milliamp to tens of amp depending on the applications. They generally consist of a regulator (or controller with discrete Mosfets), a metal composite inductor, and some auxiliary components. As a necessary part in the buck converter, the metal composite inductor takes about 1/5~1/3 of the whole volume. The substrate of the integrated power modules are made of PCB or lead frame, taking about 1/10 of the whole volume. They are packaged by plastic with all the components inside. The left space of the power modules are filled with plastic material, resulting in inefficient overall utilization of space and higher thermal resistance from the heat sources to the ambient from the top side. Generally, to guarantee enough high power density, heat sink is not applicable for these converters, then thermal issue becomes a big challenge since all the components are completely integrated in one block and heat is hard to be dissipated from the top side. However, more effort should be done by reducing the loss and reducing the thermal resistance from the heat sources to the ambient on the top side.

A new idea is proposed to package the converter with customized magnetic component which is not only the inductor but also the case of the power module. With this package and integration technology, the thermal performance of the integrated power module can be significantly improved. Section II of the paper illustrates the structure and thermal model of the power module; Section III will analyze the thermal effect of the winding loss and do a comparison with the plastic solution; Section IV shows a prototype and evaluates its performance; Section V concludes the paper.

II. STRUCTURE AND THERMAL MODEL

In this section, the detailed structure and material characteristics of the power module are presented based on which analytical thermal model is further developed. Figure 1(a) shows the structure of the magnetic core and the DC/DC converter. The converter is composed of two parts. One part is a magnetic core on the top; the other part is PCB substrate at the bottom. The terminal of the windings are soldered on the PCB substrate while some thermal conductive glue is used to provide thermal conductive path from the top of the regulator to the ceiling of the cavity. Since general magnetic material has

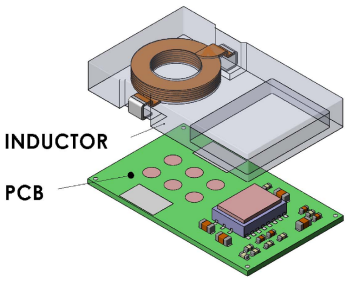

. (a) Structure of the power module.

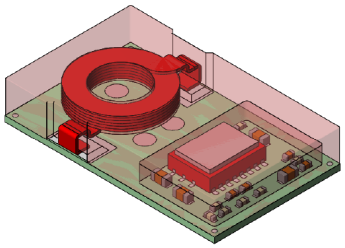

(b) Heat sources of the power module.

Fig. 1. Magnetic packaged power module

better thermal conductivity, compared with plastic packaging material used in conventional power module with a small metal composite inductor inside, the proposed magnetic packaged power module has a higher thermal conductive case, which will in turn improve the performance of the whole power module. In the proposed module, there are three major components of loss: IC loss, winding loss, and core loss. The heat generated by the loss power has two major paths to dissipate to the ambient. The first one is PCB board underneath; the second one the magnetic core on the top. Figure 1(b) shows the heat sources and the major paths for dissipating the heat to ambient. A standard four-layer board with 80×60mm size is used to dissipate the heat from the power module to the PCB board.

With the purpose of comparison, a module with the same package size but based on conventional plastic packaging is also built. Figure 2 shows the structure and distribution of the heat sources in the plastic packaged power module. Since enough space has to be left for injecting epoxy materials, the inductor in the module can't be the same size as the magnetic packaged power module in which the inductor has the same width of the module. Therefore, the inductor in plastic packaged power module is subject to having higher DCR or lower inductance value. The heat sources in plastic packaged power module are the IC die and the inductor. Compared with the proposed magnetic packaged power module, the conventional plastic power module also has two paths to dissipate the heat. One is PCB substrate at the bottom; the other one is the epoxy on the top. Very thick epoxy is injected on the top of the die as well as the inductor which make the heat dissipation less efficient than the magnetic packaged power module. The other heat dissipation path has nearly the same thermal resistance as in the magnetic packaged power module. Table I shows the definition of thermal resistance in both Figure 1 and Figure 2. To calculate the thermal resistance in both models, thermal characteristics of different materials are

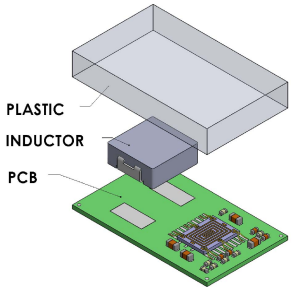

(a) Structure of the power module.

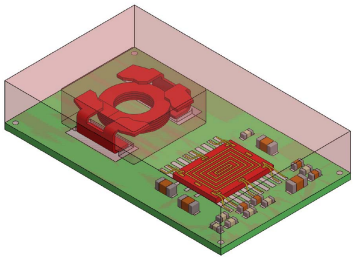

(b) Heat sources of the power module.

Fig. 2. Palstic packaged power module

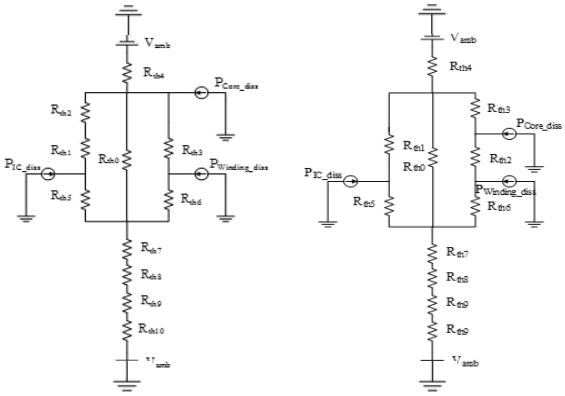

(a) Integrated power module (b) plastic packaged module

Fig. 3. thermal model of the two power modules

listed in TABLE II. With above parameters, thermal models of the both power modules can be obtained. Figure 3 shows the thermal model of the two power modules. Further loss thermal analysis will be done based on it. Thermal resistance value in the thermal models are obtained through FEA simulation. Both the proposed magnetic packaged power module and the plastic package power module have complicated internal structure. Components such as the magnetic case and the inductor winding do not have regular shapes. Therefore, it is very difficult to calculate the thermal resistance through analytical equations. However, with the help of the simulation, we can easily get the thermal resistance in an easier way. 3D simulation modules are built to calculate the thermal resistance. Thermal conductivity parameters used in

TABLE I. A. THERMAL RESISTANCE IN MAGNETIC PACKAGED POWER MODULE

Designator	Thermal resistance	Value (K/W)
R_{th1}	IC plastic thermal resistance, from the IC die to its plastic case	148
R_{th2}	Red glue thermal resistance, from the IC case to the magnetic case	2
R_{th3}	Winding insulation layer thermal resistance, from the copper to the magnetic case	3.5
R_{th4}	Magnetic case thermal resistance, from the magnetic case to the ambient	170
R_{th5}	Joints thermal resistance of the IC, from the IC die to the substrate of the module	1.2
R_{th6}	Joints thermal resistance of the inductor, from the winding to the substrate of the module	14.5
R_{th7}	Substrate thermal resistance, from the top of the substrate to the bottom of the substrate	1
R_{th8}	Joints thermal resistance of the module, from the bottom of the module to the Test board	0.5
R_{th9}	Thermal board resistance, from the top of the thermal board to ambient	2

TABLE I. B. THERMAL RESISTANCE IN PLASTIC PACKAGED POWER MODULE

Designator	Thermal resistance	Value (K/W)
R_{th1}	Thermal resistance of IC top plastic, from the IC die to the top surface of plastic case	244
R_{th2}	Winding insulation layer thermal resistance, from the copper to the magnetic case	17.6
R_{th3}	Thermal resistance from the inductor to the top surface of plastic case	223
R_{th4}	Thermal resistance of the plastic case, from the plastic case to the ambient	170
R_{th5}	Joints thermal resistance of the IC, from the IC die to the substrate of the module	4.2
R_{th6}	Joints thermal resistance of the inductor, from the winding to the substrate of the module	12
R_{th7}	Substrate thermal resistance, from the top of the substrate to the bottom of the substrate	1
R_{th8}	Joints thermal resistance of the module, from the bottom of the module to the Test board	0.5
R_{th9}	Thermal board resistance, from the top of the thermal board to ambient	2

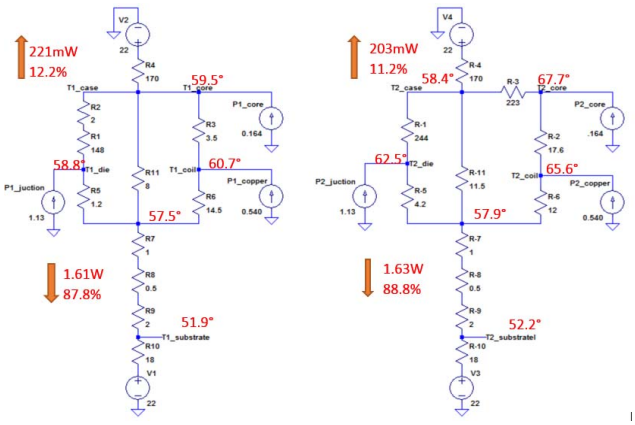

(a)Magnetic packaged module (b) Plastic packaged module

Fig. 4. Simulation results of thermal models

TABLE II. THERMAL CONDUCTIVITY OF THE MATERIALS

Materials	Thermal conductivity(W/K.m)
FR4	0.35
Epoxy	0.6
Copper	400
Red glue	1
Magnetic core	3
Solder	62

the simulation are listed in TABLE II. In the simulation, any component can be assigned as a heat source. Suppose heat flowing through a neighbor component of the source is P_{diss}, and temperature differences of the external surface and internal surface of the component is obtained in the simulation. The thermal resistance of the component can be calculated by (1). In this way, all the thermal resistance are obtained, and they are added in TABLE I, too.

$$R_{th} = \frac{\Delta T}{P_{diss}} \tag{1}$$

The thermal module is then put into a Spice software to do simulation, Figure 4 shows the temperature of different layers and the heat dissipation through each way. It can be seen that proposed power module has lower junction temperature and case temperature benefiting from its package technology.

III. LOSS AND THERMAL ANALYSIS

In this section, loss of the converter is firstly analyzed and the thermal effect is simulated through the FEA simulation. Loss of the inductor is mainly determined by the parameters of the winding. Therefore, the winding parameters will be swept to simulate its effect on thermal performances of the whole converter. The analytical thermal models have shown the proposed inductor has smaller thermal resistance from heat sources to the ambient than that of power module packaged based on conventional plastic packaging technology. Besides this benefit, the proposed inductor also has larger inductor size than the inductor used in conventional plastic packaging technology. Therefore, the inductor can have much smaller copper loss. Details about how to design the inductor are discussed in another paper. This paper only addresses the effect of loss and thermal performances of the inductor by the parameters. The inductance value L, DCR with coil radius R, coil width *w*, and wire thickness t as parameters are analyzed by FEA simulation. Figure 5 shows the inductance value versus radius and width of the inductor. Figure 6 shows the DCR versus radius and width of the inductor. According to figure 5, higher inductance value could be obtained with smaller width and larger radius winding. However, as shown in Figure 6, the DCR will also increase with this kind of parameter configurations which will result in more copper loss and higher temperature. From the perspective of thermal performance, there should be a tradeoff between inductance value and DCR. Therefore, L/R is defined as a new parameter

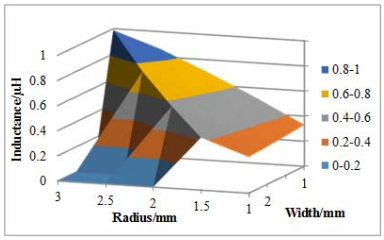

(a) Wire thickness t= 0.1

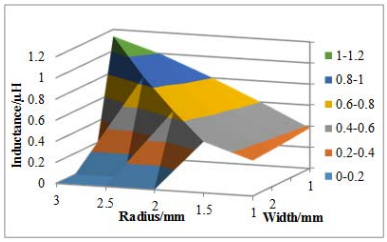

(b) Wire thickness t= 0.15

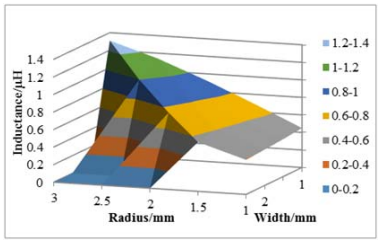

(c) Wire thickness t= 0.2

Fig. 5. Inductance value versus radius and width.

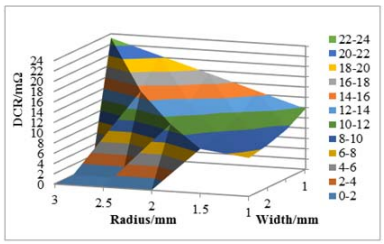

(a) Wire thickness t= 0.1

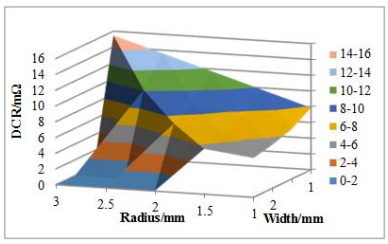

(b) Wire thickness t= 0.15

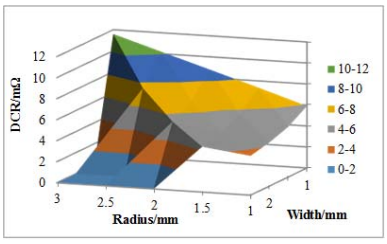

(c) Wire thickness t= 0.2

Fig. 6. DCR versus radius and width.

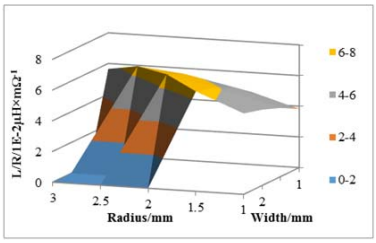

(a) Wire thickness t= 0.1

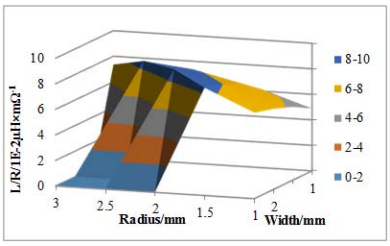

(b) Wire thickness t=0.15

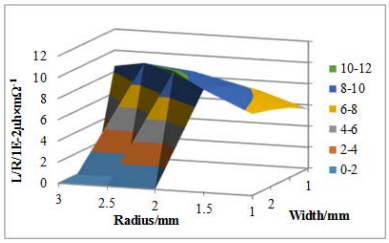

(c) Wire thickness t=0.2

Fig. 7. L/R versus radius and width.

to select the right radius, height and width to simulate the thermal effect and temperature. Figure 7 shows the L/R value with radius and width as parameters.

It can be seen that the reasonable designs for different wire thickness are around (R=1.5~2.5mm, *w*=1~2mm). So several groups of the parameters are picked out from these configurations to simulate the thermal effect of winding parameters. They are show in Table III. Thermal performance of the proposed power module is simulated based on the losses of different winding configurations. The results are shown in Figure 8. It can be seen the winding parameter of the inductor also plays an important role on the thermal performances of the whole converter. With different parameters, the DCR differentiates a lot, and thus the winding loss, which can result in 4℃ different on the case.

Although Group 3 in Table III has only 5.8mΩ DCR value, the winding can't be used in the inductor since the total thickness of the winding is too thick, leaving very thin magnetic material on top and bottom. Also, it is not practical from the perspective of the manufacturing. In the following analysis, Group 2 will be chosen to do comparison. As discussed in last section, benefiting from the larger space for the inductor winding in the proposed module, either higher inductance or lower DCR can be achieved. In other words, the inductor used in plastic packaging will have either lower inductance or higher DCR value since its volume is smaller than the proposed inductor for leaving enough space to do plastic packaging. In this paper, a commercial inductor with 5×5×2.2mm size, 1μH inductance value is selected to do the comparison. Its DCR value is 17mΩ. The selected inductor is soldered on the same substrate of the proposed power module and then packaged with plastic material to do comparison. Another power module with same DCR value but different package is also simulated to see the effect of packaging itself on thermal. Both the power modules are simulated to show their thermal performances in the software.

TABLE III. LOSS VS INDUCTOR CONFIGURATION

Groups	Thickness (mm)	Width (mm)	Radius (mm)	DCR (mΩ)	Loss (mW)
Group 1	0.1	1	2.5	17.6	752
Group 2	0.15	1	1.8	11.7	500
Group 3	0.2	1	1.5	5.8	248

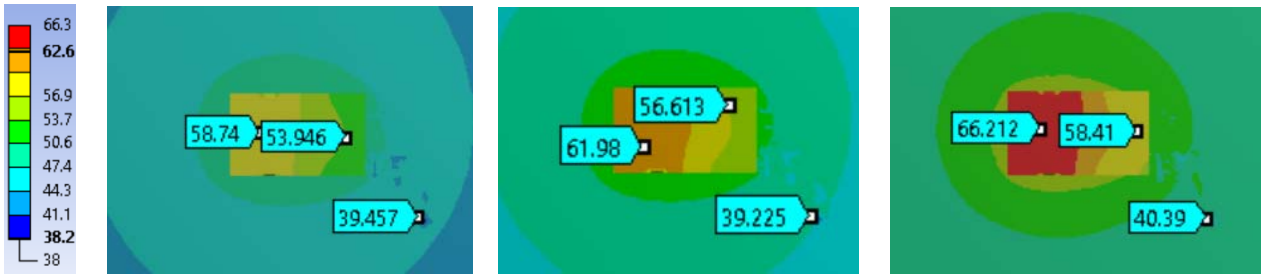

(a)DCR=5.8mΩ, copper loss=248mW; (b) DCR=11.7mΩ, copper loss=500mW; (c) DCR=17.6mΩ, copper loss=752mW.

Fig. 8. Thermal simulation results of magnetic packaged power modules with different winding configuration. (a) *t*=0.2mm, *R*=2mm, *w*=1.5mm; (b) *t*=0.15mm, *R*=1.5mm, *w*=1.2mm; (c) *t*=0.1mm, *R*=1.5mm, *w*=1mm.

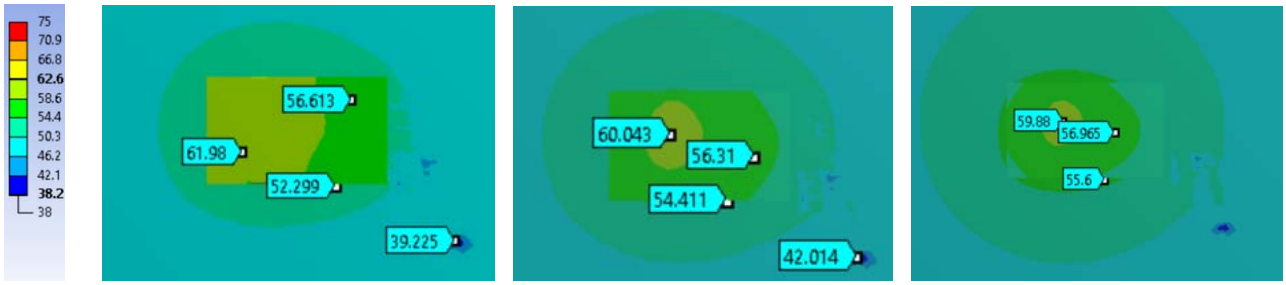

(a) Magnetic packaged module, DCR=11.7mΩ; (b) plastic packaged module, DCR=11.7mΩ; (c) plastic packaged module, DCR=17.6mΩ

Fig. 9. Case thermal plots for magnetic and plastic packaged modules.

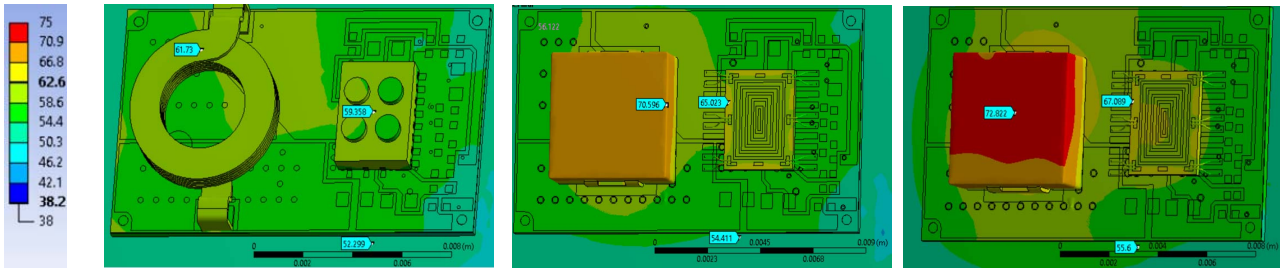

(a) Magnetic packaged module, DCR=11.7mΩ; (b) plastic packaged module, DCR=11.7mΩ; (c) plastic packaged module, DCR=17.6mΩ

Fig. 10. Junction thermal plots for magnetic and plastic packaged modules.

A 3D FEA simulation is used to calculate the power loss, based on which further thermal analysis is executed. A test is set up to measure the thermal conductivity coefficient of the magnetic core. The result is 3W/m-k, which is 5 times of the value for plastic packaging material 0.6W/m-k. With the thermal conductivity coefficient, a thermal simulation is also executed to show the thermal effect of inductor loss determined by different dimension configurations. In the thermal simulation, the module is soldered on an 80×60mm four layer PCB board to help dissipate the heat. Figure 9 and 10 shows the case and junction thermal plots of the power module at full load (6A). According to the results, junction temperature of magnetic package can be 11°C lower (61.7°C compared with 72.8°C). By considering several factors, such as the physical size limitation, power loss, saturation current, the specification of the inductor is chosen to be w=1.2mm, t=0.15mm, R=1.75mm for making prototypes.

IV. Prototype and Test

In this section, a prototype of the proposed power module is made to test its performances. The power module is composed of an inductor on the top and the PCB substrate at the bottom. A regulator together with some auxiliary components is soldered on the PCB (underneath the inductor cavity). Figure 11 shows the picture of the inductor, and the winding used for making the inductor. A 5.5 turn winding is used in the inductor. The winding is formed with 1.2×0.15mm planar copper wire with the purpose of reducing the eddy current loss. The whole inductor has the size of 15×9×2.4mm and the winding is embedded on one side of the inductor, leaving a 6×5×1mm cavity on the other side to put the components underneath. Figure 12 shows the schematic of the power module, top and bottom views of the assemble power module. The power module is then soldered on an evaluation board to do further

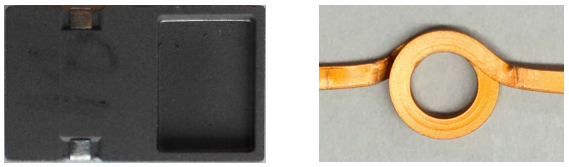

(a) Inductor (bottom view). (b) Winding.

Fig. 11. Picture of the inductor and the winding

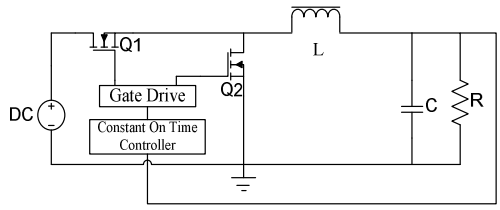

(a) Schematic

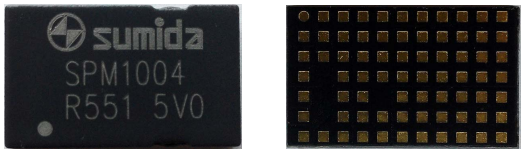

(b) Top view. (c) Bottom view.

Fig. 12. Schematic and picture of the power module.

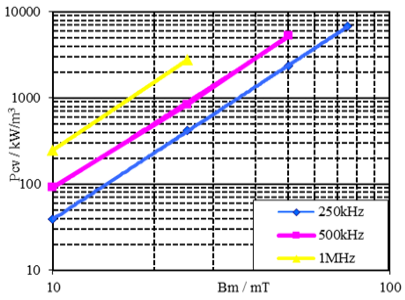

Fig. 13. Loss character of magnetic material

measurement and analysis. The power module operates under the constant on time control with the purpose of high light load efficiency. To do loss break down of the converter, the loss character of the magnetic material is measured, it is shown in Figure 13. Core loss is then simulated with FEA software by extracting the parameters based on the loss character curves. The core loss is much smaller than the winding loss since the major output current component is DC. Based on the inductor loss analysis, Total loss breakdown is executed to show loss distribution of the power module. The results are shown in Figure 14.

Benefiting from the higher thermal conductivity of the iron powder and high efficiency regulator, the magnetic packaged converter has better thermal performance than its plastic packaging counterparts. A thermal evaluation board is made to evaluate the prototype and the other two plastic packaging power modules with the same input and output specifications. Figure 15 shows the comparison of efficiency curves between the proposed power module and plastic packaged power module with same DCR and substrate. For the two plastic packaged power modules, #3 has the same size as the prototype; the other one has bigger size of 15×15×2.8mm. Figure 16 shows the comparison of efficiency curves between the 3 power modules. They are soldered on the thermal evaluation board with the same copper area as the prototype is. All the three power modules have the 12V input, 5V/6A output. Figure 17 shows the picture of the thermal evaluation board and the thermal image when the output power is 30W (5V/6A). It can be observed that the prototype has the same temperature with the bigger size power module (#2), and 11 ℃ less than the power module with the same size (#1). Without the outer plastic package layer, the magnetic packaged power module has bigger inductor volume and less thermal resistance from the heat sources to ambient. To show this benefit, loss analysis of three power modules is executed and the corresponding contributions to temperature rise are calculated. Table IV shows the results. The prototype has the same temperature rise with #2 although it has smaller volume. The prototype has less temperature rise than #3 because it has less inductor loss and better heat dissipating condition.

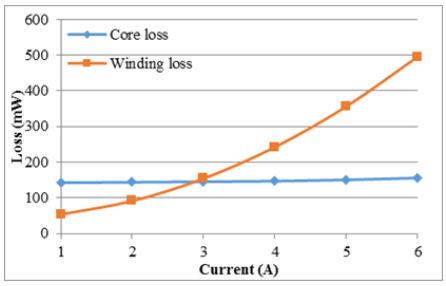

Fig. 14. Total loss break down

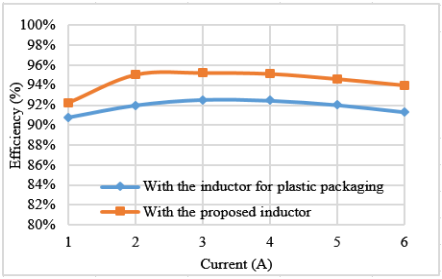

Fig. 15. Efficiency curves for proposed power modules and plastic packaged power module with same DCR and substrate

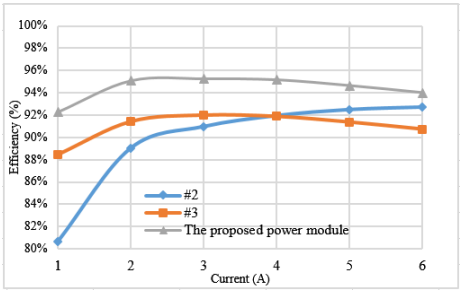

Fig. 16. Efficiency curves for three different power modules

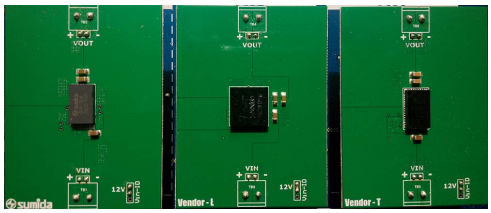

(a) Thermal board

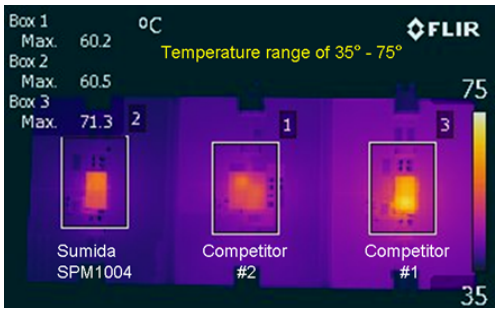

(b) Thermal imagine

Fig. 17. Thermal board picture and the thermal image.

TABLE IV. INDUCTOR LOSS AND ITS CONTRIBUTION TO TEMPURETURE RISE

	Prototype (SPM1004)	**#2**	**#3**
Inductor loss (W)	0.82	0.81	1.02
Temperature rise (℃)	15.1	15.3	19.6

V. CONCLUSION

This paper analyses the thermal performance of the magnetic packaged power module. Benefiting from the high thermal conductivity of the magnetic material, the power module has less thermal resistance from the heat source to ambient, thus better thermal performance. Compared with the plastic packaging, the magnetic packaged power module has less case temperature and higher efficiency. Detailed analysis on how much the magnetic package can enhance the thermal performance has also been presented.

REFERENCES

[1] Ke Ma; Bahman, A.S.; Beczkowski, S.; Blaabjerg, F., "Complete Loss and Thermal Model of Power Semiconductors Including Device Rating Information," in Power Electronics, IEEE Transactions on , vol.30, no.5, pp.2556-2569, May 2015.

[2] Shuojie She; Wenli Zhang; Xiucheng Huang; Weijing Du; Zhengyang Liu; Lee, F.C.; Qiang Li, "Thermal analysis and improvement of cascode GaN HEMT in stack-die structure," in Energy Conversion Congress and Exposition (ECCE), 2014 IEEE , vol., no., pp.5709-5715, 14-18 Sept. 2014

[3] Isidoril, A.; Rossi, F.M.; Blaabjerg, F.; Ma, K., "Thermal Loading and Reliability of 10-MW Multilevel Wind Power Converter at Different Wind Roughness Classes," in Industry Applications, IEEE Transactions on , vol.50, no.1, pp.484-494, Jan.-Feb. 2014.

[4] Josifovic, I.; Popović-Gerber, J.; Ferreira, J.A., "Thermal management of compact SMT multilayer power converters," in Energy Conversion Congress and Exposition (ECCE), 2011 IEEE , vol., no., pp.52-59, 17-22 Sept. 2011

[5] Gautam, D.; Wager, D.; Musavi, F.; Edington, M.; Eberle, W.; Dunford, W.G., "A review of thermal management in power converters with thermal vias," in Applied Power Electronics Conference and Exposition (APEC), 2013 Twenty-Eighth Annual IEEE , vol., no., pp.627-632, 17-21 March 2013

[6] Senturk, O.S.; Helle, L.; Munk-Nielsen, S.; Rodriguez, P.; Teodorescu, R., "Converter Structure-Based Power Loss and Static Thermal Modeling of The Press-Pack IGBT Three-Level ANPC VSC Applied to Multi-MW Wind Turbines," in Industry Applications, IEEE Transactions on , vol.47, no.6, pp.2505-2515, Nov.-Dec. 2011.

[7] Seung-Yo Lee; Pfaelzer, A.G.; van Wyk, J.D., "Thermal analysis for improved packaging of 4-channel 42 V/14 V DC/DC converter," in Industry Applications Conference, 2004. 39th IAS Annual Meeting. Conference Record of the 2004 IEEE , vol.4, no., pp.2330-2336 vol.4, 3-7 Oct. 2004.

[8] Gerstenmaier, Y.C.; Castellazzi, A.; Wachutka, G.K.M., "Electrothermal simulation of multichip-modules with novel transient thermal model and time-dependent boundary conditions," in Power Electronics, IEEE Transactions on , vol.21, no.1, pp.45-55, Jan. 2006

[9] Cheng, M.-C.; Feixia Yu, "Heat flow models for silicon-on-insulator structures," in Electron Devices for Microwave and Optoelectronic Applications, 2003. EDMO 2003. The 11th IEEE International Symposium on , vol., no., pp.244-249, 17-18 Nov. 2003.

[10] DeVoe, J.; Ortega, A., "An investigation of board level effects on compact thermal models of electronic chip packages," in Semiconductor Thermal Measurement and Management, 2002. Eighteenth Annual IEEE Symposium , vol., no., pp.8-14, 12-14 March 2002.